Nanoparticles Targeting Dendritic Cell Surface Molecules Effectively Block T Cell Conjugation and Shift Response

Chuda Chittasupho,[†] Laura Shannon,[‡] Teruna J. Siahaan,[†] Charlotte M. Vines,[‡] and Cory Berkland[†,§,*]

[†]Department of Pharmaceutical Chemistry, University of Kansas, Lawrence, Kansas 66047, United States, [‡]Department of Microbiology, Molecular Genetics and Immunology, University of Kansas Medical Center, Kansas City, Kansas 66160, United States, and [§]Department of Chemical and Petroleum Engineering, University of Kansas, Lawrence, Kansas 66047, United States

ABSTRACT Dendritic cells (DCs) are potent professional antigen presenting cells (APC) that activate naïve T cells. Interaction of ICAM-1 and LFA-1 molecules on each cell is required for T cell conjugation to DCs, which leads to naïve CD4+ T cell activation and proliferation. Nanoparticles capable of blocking LFA-1/ICAM-1 interaction were studied as inhibitors of T cell conjugation to DCs. Primary DCs were primed with ovalbumin, then treated with a peptide that binds ICAM-1 (LABL), a peptide that binds LFA-1 (cIBR), or the same peptides covalently linked to the surface of poly(DL-lactic-*co*-glycolic acid) nanoparticles (NPs). LABL-NPs and cIBR-NPs rapidly bound to DCs and inhibited T cell conjugation to DCs to a greater extent than the free peptides, unconjugated nanoparticles (NPs), anti-ICAM-1 antibodies, and anti-LFA-1 antibodies. In addition, DCs treated with NPs or with cIBR-NPs stimulated the proliferation of T cells, but DCs treated with LABL-NPs did not stimulate T cell proliferation. Nanoparticles targeting ICAM-1 or LFA-1 also altered cytokine production by DC cocultured with T cells when compared to free ligands, suggesting that these NPs may offer a unique tool for shaping T cell response.

KEYWORDS: peptides · nanoparticles · targeted delivery · dendritic cells · T cell

Professional antigen presenting cells (APCs) such as dendritic cells (DCs) help orchestrate immune responses to foreign antigens by capturing antigen and loading it onto major histocompatibility complex (MHC) class II. The antigen-primed APCs then present the antigen to naïve CD4+ T cells which express cognate T cell receptors.[1] The resulting immunological synapse formed between T cells and APCs often initiates signaling events for T cell proliferation and effector function such as cytokine production.[2] Leukocyte function-associated antigen-1 (LFA-1; primarily on T cells) binding to intercellular adhesion molecule 1 (ICAM-1; primarily on DCs) can prolong the immunological synapse and support T cell activation.[3−5] Targeting of these molecules is known to modify T cell activation.[6]

Molecules that mediate cell adhesion or signaling are typically present in large numbers at the cell−cell interface. Several studies have shown that multivalency can enhance the binding of ligands to these types of receptors and shift the response of targeted cells.[7−10] For example, multivalent presentation of anti-CD20 monoclonal antibody fragments can enhance the targeting of B cell antigen CD20.[10] Similarly, multiple copies of peptide ligands on a polymer backbone can improve binding to CD21 on B cells when compared to free ligand.[11]Arrays of RGD peptides on micelles have been consistently found to dramatically enhance binding to $\alpha_v\beta_3$ integrins in contrast to free RGD peptides.[12]

The response of cells targeted by multivalent ligands is often unexpected. Antigen valency has been found to be a key parameter affecting binding to B cells and cellular response.[13] High valency antigen arrays induced antibody production by B cells, while low valency antigen arrays did not.[13] Multivalent ligands induced calcium influx in a dose-dependent manner, whereas the same molar concentration of free ligand did not.[13] Ligand valency also affects the response of leukocytes undergoing rolling adhesion. For example, multivalent L-selectin ligands clustered L-selectin and induced L-selectin shedding, but the corresponding monovalent ligands did not.[14,15] Thus, multivalent ligands can affect cell response in addition to enhancing ligand binding.

The binding of LFA-1 and ICAM-1 is also controlled by changes in avidity resulting from receptor clustering.[16,17] Cell adhesion mediated by ICAM-1 and LFA-1 involves multivalent interaction between these two molecules on opposing cells (APC and T cell). LABL (ITDGEATDSG) is a peptide modeled after the I domain of LFA-1, which is the binding site of ICAM-1. The cIBR (cyclo 1,12 Pen-PRGGSVLVTGC) is a cyclic peptide derived from domain 1 of ICAM-1 which binds

* Address correspondence to berkland@ku.edu.

Received for review August 25, 2010 and accepted February 14, 2011.

Published online March 04, 2011
10.1021/nn102159g

TABLE 1. Nanoparticle Properties of Specified Formulations[a]

	NP	LABL-NP	cIBR-NP
effective diameter (nm)	154.6 ± 10.0	172.6 ± 2.5	171.9 ± 4.3
polydispersity	0.026 ± 0.030	0.070 ± 0.039	0.055 ± 0.005
zeta-potential (mV)	−21.4 ± 0.4	−34.7 ± 2.0	−13.9 ± 0.8

[a] Values are representative of three experiments (mean ± SD).

TABLE 2. Density of Peptides on the Surface of Nanoparticles[a]

	size (nm)	total surface area (m^2/g of PLGA)	peptide density (pmol/cm^2)
LABL-NP	172.6	25.9	265.5 ± 78.5
cIBR-NP	171.9	26.1	39.5 ± 3.0

[a] Values are representative of three experiments (mean ± SD).

to the I domain of LFA-1.[18,19] LABL and cIBR peptides inhibit homotypic and heterotypic T cell adhesion as well as mixed lymphocyte reactions.[20−22]

Nanoparticles modified with these peptides (cLABL-NPs and cIBR-NPs) were previously used to specifically target ICAM-1 and LFA-1 expressing cells, respectively.[23−25] NPs targeting these receptors were found to bind cells and rapidly internalize *via* receptor-mediated endocytosis. In addition, cIBR-NP blocked the adhesion of T cells to lung epithelial cells expressing a high level of ICAM-1.[23] Since the oligomeric states of LFA-1 and ICAM-1 molecules contribute to their ability to regulate T cell responses, it was hypothesized that these nanoparticles may bind with high avidity to ICAM-1 or LFA-1 on DCs. Such targeted NPs were suspected to be better inhibitors of T cell conjugation to DCs compared to free ligands and a potential tool to alter cell response.

RESULTS

Characterization of Nanoparticles and Peptide-Conjugated Nanoparticles. A variety of targeted and control NPs were synthesized. The size of all PLGA NP formulations was less than 200 nm, and NPs possessed a negative zeta-potential (Table 1). Low polydispersity values (<0.1) suggested a relatively narrow particle size distribution. LABL and cIBR peptides were successfully conjugated to PLGA-NPs. The zeta-potential of LABL-NPs was more negative than unconjugated NPs, presumably due to the LABL peptide having a net charge of −3. cIBR-NPs had a less negative charge than unconjugated NPs. Pluronic-COOH groups were probably masked by the cIBR peptide, which has a net charge of +1. The amounts of LABL and cIBR peptides attached to NPs were determined by quantifying the unconjugated peptide remaining in the medium after the conjugation reaction.[23] LABL was conjugated with a high density, while cIBR density closely matched a previous publication (Table 2).[23]

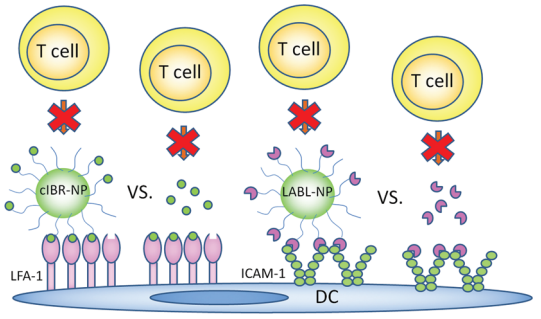

Figure 1. T cell conjugation to DCs may be blocked by the binding of cIBR-NP to LFA-1 or LABL-NP to ICAM-1 on DCs.

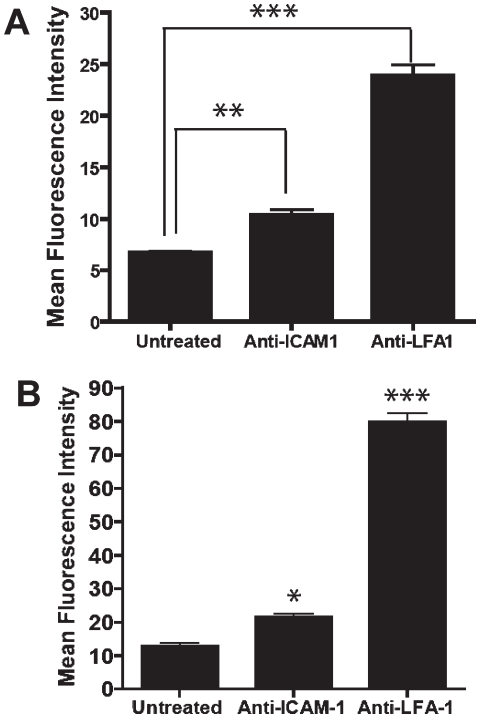

Figure 2. (A) ICAM-1 and LFA-1 expression on dendritic cells and on (B) T cells. OVA-primed DCs and T cells were incubated with anti-ICAM-1 and anti-LFA-1 for 45 min on ice. Cells were washed and analyzed by flow cytometry; * indicates $p < 0.05$, ** indicates $p < 0.01$ and * indicates $p < 0.001$.**

Relative Expression of ICAM-1 and LFA-1 on DCs and T Cells. Expression levels of ICAM-1 and LFA-1 on activated bone marrow derived dendritic cells (DCs) matured with TNF-α and primed with ovalbumin (OVA) were determined using fluorescent anti-ICAM-1 and anti-LFA-1. DCs expressed both ICAM-1 and LFA-1, indicating that either LABL or cIBR could be used to target these adhesion molecules on DCs (Figure 2A). For these studies, we used primary CD4+ T cells, which express an ovalbumin specific T cell receptor (OT-II T cells isolated from B6.129S7-*Rag1*^{tm1Mom} Tg(TcraTcrb) 425Cbn mice). Flow cytometry data showed minimal expression of ICAM-1 on primary OT-II T cells but high expression of LFA-1 as expected (Figure 2B). Although NPs were not directly

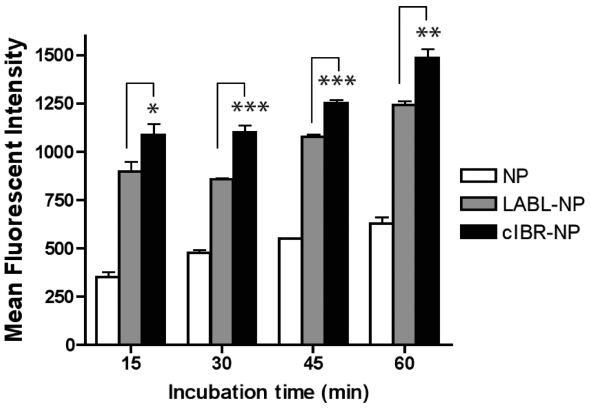

Figure 3. Binding of NPs, LABL-NPs, or cIBR-NPs to dendritic cells. NPs, LABL-NPs, and cIBR-NPs were incubated with OVA-primed and TNF-α-activated DCs for 15, 30, 45, or 60 min at 37 °C and analyzed by flow cytometry. The interaction of cIBR-NPs with dendritic cells was significantly greater than LABL-NPs and untargeted NPs at all time points. The fluorescence of dendritic cells incubated with each of the NP types increased with time; * indicates $p < 0.05$, ** indicates $p < 0.01$, and * indicates $p < 0.001$.**

incubated with OT-II T cells, the relative expression of these two receptors was provided for reference.

Both LABL-NPs and cIBR-NPs Exhibited Rapid Binding to DCs. LABL peptide binds specifically to the domain 1 of ICAM-1, whereas cIBR peptide binds the I domain of LFA-1.[18,19] LABL-NPs, cIBR-NPs, and unconjugated NPs were incubated with DCs to investigate the binding by DCs. Immature DCs were stimulated with TNF-α and primed with OVA for 24 h prior to addition of NPs. In comparison to untargeted NPs, fluorescence intensities of DCs incubated with LABL-NPs or cIBR-NPs were much higher than cells incubated with untargeted NPs at all incubation times. Fluorescence intensities of DCs incubated 45 min with LABL-NPs or cIBR-NPs were ~2- and ~2.3-fold greater than NPs, respectively, indicating that the interactions of LABL-NPs and cIBR-NPs with DCs occurred more rapidly and to a greater extent compared to untargeted NPs (Figure 3).

Fluorescence Microscopy of DC Binding Nanoparticles. The binding of NPs, LABL-NPs, or cIBR-NPs by DCs was also followed using fluorescence microscopy. Nanoparticle fluorescence rapidly localized to DCs (Figure 4A). Images collected using MetaMorph were analyzed using ImageJ software and showed ~2 times greater fluorescence intensity of DCs incubated with LABL-NPs compared to untargeted NPs at 40 min (Figure 4B), thus supporting flow cytometry results. DCs treated with cIBR-NPs demonstrated even higher fluorescent intensities. These results indicated that LABL-NPs and cIBR-NPs effectively targeted DCs.

The internalization of LABL-NPs and cIBR-NPs was supported by the punctate fluorescence pattern observed in the micrographs. Similar patterns were also reported for the uptake of untargeted NPs and cLABL-NPs in lung epithelial cells (A549 cells) and endothelial cells (HUVECs) expressing high levels of ICAM-1 in previous

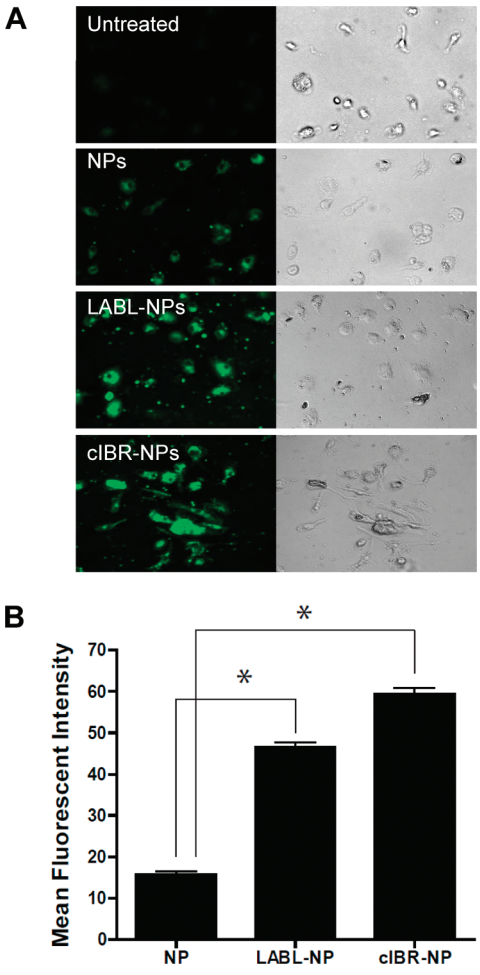

Figure 4. (A) Fluorescent micrographs of DCs in medium (untreated), DCs incubated with untargeted NPs, DCs incubated with LABL-NPs, and DCs incubated with cIBR-NPs for 40 min. Punctate fluorescence patterns suggested the accumulation of NPs with the cells. (B) Mean fluorescent intensities of DCs incubated with NP, LABL-NP, and cIBR-NP were quantified from micrographs using ImageJ software. DCs were stimulated by TNF-α and primed with OVA for 24 h prior to the study. DCs were then incubated with NPs, LABL-NPs, and cIBR-NPs for 40 min at 37 °C; * indicates $p < 0.001$.

reports.[24,25] The punctate pattern of cIBR-NPs appeared slightly more evident than LABL-NPs and untargeted NPs at 40 min of incubation (Figure 4A). These results supported the flow cytometry data.

***In Vitro* Cellular Cytotoxicity of LABL-NPs or cIBR-NPs.** Cell viability studies indicated that LABL-NPs and cIBR-NPs were minimally cytotoxic to DCs and T cells. The average cell viability was greater than 95% at all concentrations tested when LABL-NPs and cIBR-NPs were incubated with DCs for 24 h (Figure 5A,B). For reference, the viability of T cells exposed to LABL-NPs and cIBR-NPs relative to untreated cells was also evaluated. After 24 h of treatment, a decrease in T cell viability was observed at LABL-NPs concentrations higher than 16 mg/mL (IC_{50} = 25.6 mg/mL). The IC_{50} of cIBR-NPs with T cells was 3.4 mg/mL. From our results, we inferred that DCs were highly viable after incubation with these particles

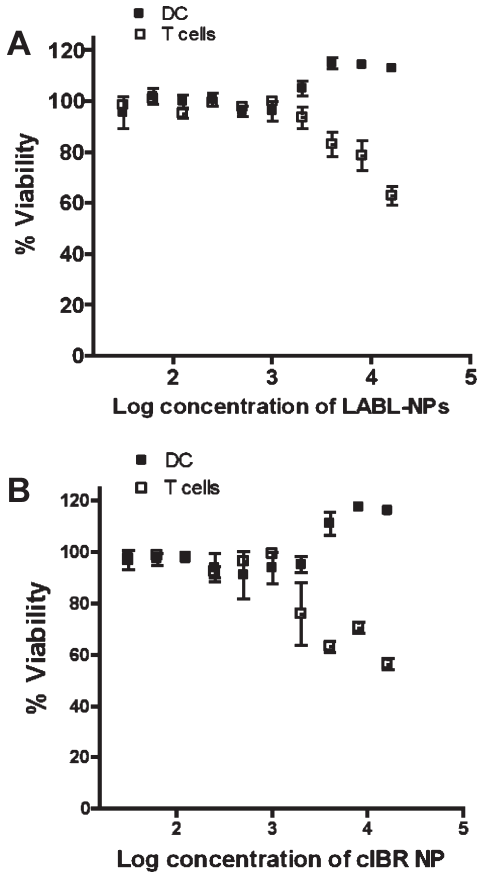

Figure 5. Dendritic cell and T cell viability in the presence of (A) LABL-NPs or (B) cIBR-NPs. LABL-NPs and cIBR-NPs were minimally cytotoxic to DCs and T cells at the concentrations used for ensuing studies.

for 30 min in the conjugation study. DC cultures were washed to remove any free NPs prior to addition of primary T cells; therefore, T cell cytotoxicity data are only offered for references.

Peptide–NPs Significantly Inhibited the Conjugation of DCs and T Cells. The induction of cell proliferation and cytokine production in resting T cells requires binding of LFA-1 on T cells and its receptor, ICAM-1, on DCs to allow prolonged signaling.[3–5] The effect of LFA-1/ICAM-1 blockade on conjugate formation between T cells isolated from B6.129S7-*Rag1*^{tm1Mom} Tg(TcraTcrb)-425Cbn mice and mature DCs primed with OVA was investigated. LABL-NP blockade of ICAM-1 on DCs led to a substantial decrease in the number of T cells bound to DCs (Figure 6). Pretreatment of DCs with LABL-NPs resulted in up to a 76% decrease in T cell binding to DCs compared to T cells incubated with untreated DCs. From these results, we inferred that LABL-NPs bound ICAM-1 expressed on DCs and blocked the availability of ICAM-1 to interact with LFA-1 on T cells. The number of T cells interacting with DCs pretreated with cIBR-NPs was decreased up to 78% compared to T cells incubated with untreated DCs. Untargeted NPs decreased the T cell conjugation to DCs by only 23%.

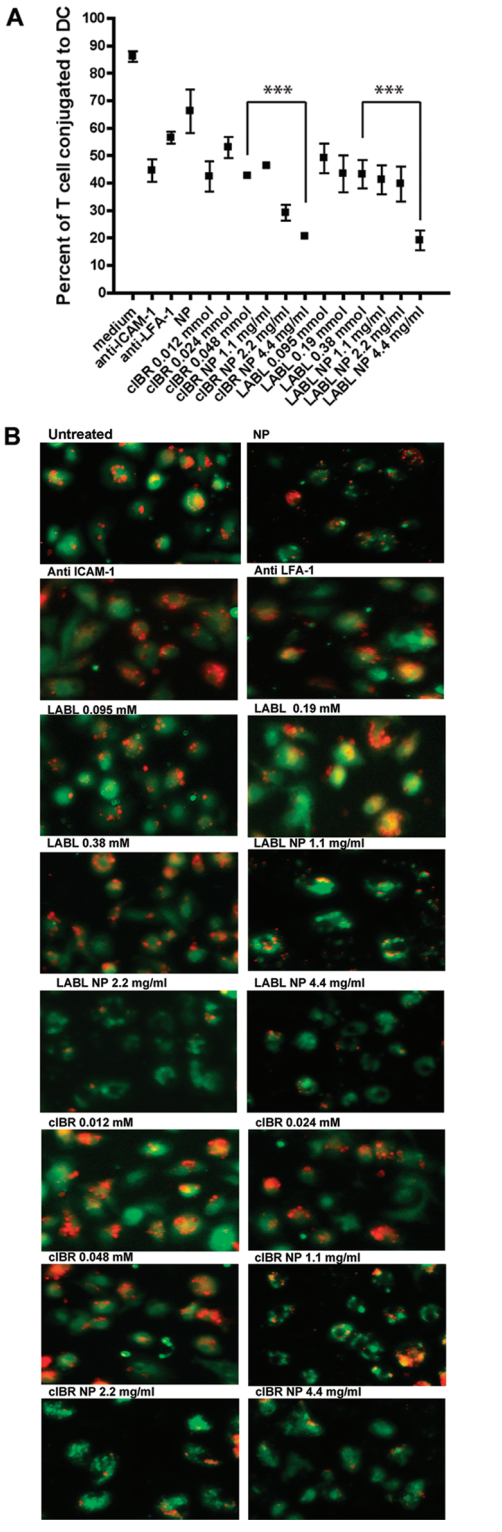

Figure 6. (A) Blocking of DC–T cell conjugate formation. LABL-NPs and cIBR-NPs inhibited the binding of T cells to DCs to a much greater extent than free LABL and cIBR peptides. (B) Micrographs of T cells (red) binding DCs (green). LABL-NPs and cIBR-NPs exhibited greater inhibition of T cell conjugation to DCs than LABL peptides, anti-ICAM-1, anti-LFA-1, NPs, and untreated DCs. DCs incubated with samples were washed and T cells were cocultured for 2 h, and T cells and DCs were imaged and counted; * indicates $p < 0.001$.**

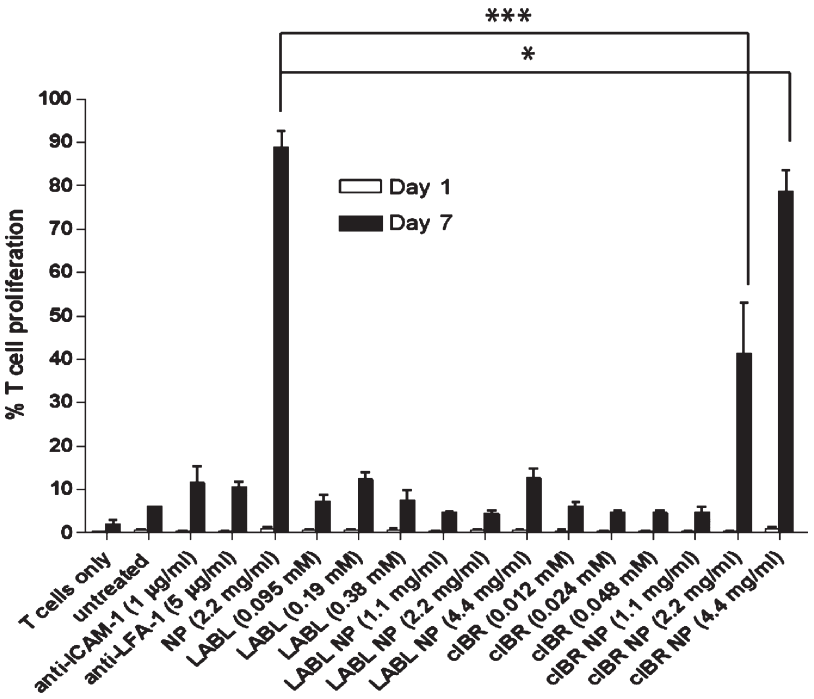

Figure 7. Proliferation of T cells after coculture with DCs treated with samples. The percent of T cells dividing after incubation for 24 h (1 day) and 168 h (7 days) was determined by flow cytometry. DCs incubated with TNFα and primed with OVA were incubated with samples for 30 min at 37 °C. After removing samples, OVA-specific T cells were added and incubated with DCs for 7 days. cIBR-NPs and untargeted NPs stimulated the proliferation of OT-II T cells, but other samples did not significantly alter T cell proliferation; * indicates $p < 0.001$ and * indicates $p < 0.05$.**

In addition, free peptides were incubated at molar concentrations corresponding to the molar amount of peptides presented on the surface of nanoparticles. Peptide-conjugated nanoparticles blocked the binding of T cells to DCs significantly better than free peptides. Furthermore, inhibition of the T cell conjugation to DCs was further enhanced by increasing LABL-NP or cIBR-NP concentration. These data were also analyzed by counting T cells conjugated to DCs (Supporting Information Figure 1), and the results were in agreement with the analysis reported here using ImageJ software.

Effects of LABL-NPs and cIBR-NPs on T Cell Proliferation. To examine the effect of NPs on T cell proliferation, carboxyfluorescein diacetate succimidyl ester (CFSE) fluorescence dilution in OVA-specific T cells was analyzed after co-incubation with DCs for 24 h (1 day) and 168 h (7 days). DCs were pretreated with untargeted nanoparticles (NPs), antibodies, free peptides, or peptide-conjugated NPs. The three different molar concentrations of free peptides matched the molar concentration of peptide conjugated to NPs. Division of cells was calculated from the percentage of cells having diluted fluorescent intensity using Flowjo software. Untargeted NPs and cIBR-NPs incubated with DCs led to a substantial increase in the number of T cells undergoing division. We observed that 89, 78, and 41% of T cells divided following co-incubation with DCs that had been pretreated with NPs (2.2 mg/mL) or cIBR-NPs (4.4 and 2.2 mg/mL) for 7 days, respectively. In contrast, T cells incubated with untreated DCs only proliferated ~6%.

The proliferation of T cells incubated with DCs pretreated with anti-ICAM-1, anti-LFA-1, LABL peptide, LABL-NPs (4.4, 2.2, and 1.1 mg/mL), or cIBR peptide was not substantially altered by the treatments (Figure 7). There were no significant differences in the levels of T cell proliferation between the groups of DCs treated with these samples when compared to untreated DCs. T cells alone without DCs were used as a negative control and yielded a T cell proliferation of only ~1.8%.

Cytokine Production of DCs and OT-II T Cells. One marker for DC maturation and T cell stimulation is the production of cytokines. Cytokines are produced by both antigen presenting cells such as DCs and by T cells. DCs predominantly produce TNF-α, IL-1, and IL-6 proinflammatory cytokines.[26] IL-2 is produced by CD4+ T cells.[27] To observe cytokine production of DCs after treatment with peptides or nanoparticles, DCs matured with TNF-α and primed with OVA were incubated with LABL peptide, cIBR peptide, LABL-NPs, cIBR-NPs, or NPs for 30 min. DC cultures were washed, and then OT-II T cells were cocultured with DCs for 7 days, and cytokine production was determined by enzyme-linked immunoassay (ELISA). DCs incubated with LABL-NPs, cIBR-NPs, or NPs secreted significantly higher amounts of TNF-α (4−5-fold), relative to untreated DCs. In contrast, the amounts of TNF-α produced by DCs treated with LABL and cIBR peptide solutions were very low, similar to untreated DCs (Figure 8A).

Furthermore, the amount of IL-6 produced by coculture of T cells with DCs pretreated with untargeted NPs

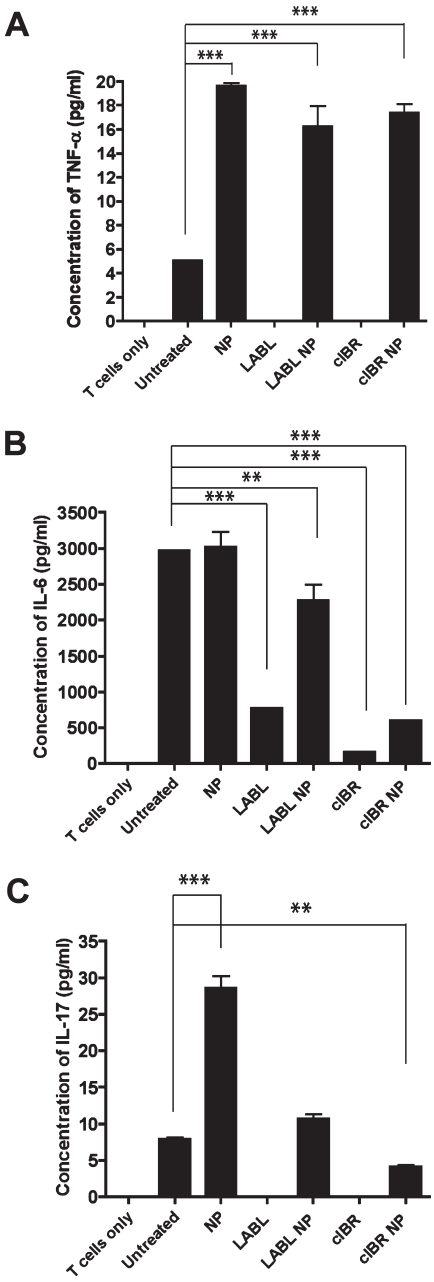

Figure 8. Production of cytokines in cocultures where DCs were pretreated with LABL-NPs, cIBR-NPs, untargeted NPs, LABL peptide, or cIBR peptide. (A) All nanoparticles increased the secretion of TNF-α compared to untreated DCs. (B) LABL-NPs, cIBR-NPs, LABL, and cIBR peptides decreased the amount of IL-6 detected in the coculture of DCs and T cells relative to untreated DCs. Untargeted NPs increased the level of IL-6 production in the coculture of DCs and T cells. (C) Untargeted NPs induced the production of IL-17 from activated OT-II T cells. LABL-NPs, cIBR-NPs, LABL, and cIBR peptides did not stimulate the production of IL-17; ** indicates $p < 0.01$ and * indicates $p < 0.001$.**

was not significantly different from the coculture of untreated DCs and T cells. Conversely, the amount of IL-6 produced by coculture of T cells with DCs pretreated with LABL peptide, cIBR peptide, LABL-NPs, or cIBR-NPs was lower than coculture of untreated DCs and T cells (Figure 8B). These results suggested that LABL peptide, cIBR peptide, LABL-NPs, and cIBR-NPs did not stimulate IL-6 production, which is predominantly produced by DCs.[26] Untargeted NPs did not alter IL-6 production relative to untreated DCs, suggesting that these particles neither bound specifically to cell adhesion molecules nor blocked the activation of the OT-II T cells.

Proliferation of naïve CD4+ T cells into effector T cells is also regulated by mature DCs. Coculture of OT-II T cells with DCs that had been preincubated with untargeted NPs enhanced T cell proliferation and production of IL-17, when compared to other treatments or controls (Figure 8C). From these results, we concluded that the presence of untargeted NPs promotes activation of T cells and may increase production of TGF-β, which is normally considered immunosuppressive. Yet, in the presence of IL-6, TGF-β promotes the expression of IL-17 and the differentiation of Th17 CD4 cells.[28] These findings are further supported by the low levels of IL-6 produced by LABL, cIBR, LABL-NP, and cIBR-NP treatments, which correlate with the production of IL-17 since IL-6 in combination with TGF-β induces Th17 differentiation from naïve CD4+ T cells.[28] Finally, the amount of IL-2 was undetectable in all media of DCs cocultured with OT-II T cells.

DISCUSSION

A critical step in the development of an immune response is the activation of T cells. This process transitions naïve CD4+ T cells into effector cells. T cell activation begins with antigen recognition through a highly specific interaction between T cell receptor (TCR) and antigenic peptide presented by major histocompatibility complex (MHC) molecules on the surface of antigen presenting cells.[1] The activation of a T cell by an APC requires the reorganization of receptors and ligands to form an immunological synapse. This dynamic and highly organized structure maintains the cell−cell interaction.[29] The immunological synapse is formed by a rearrangement of receptors that form supramolecular activation clusters. The central cluster comprises TCR−peptide−MHC interaction, which is surrounded by LFA-1 and ICAM-1 adhesion molecules, among others, in the mature immunological synapse.[30] The binding of TCRs to peptide−MHC complexes further activates LFA-1 on T cells that recognize and bind ICAM-1 on APC.[2] This interaction strengthens the conjugation of APC and T cells and completes the immunological synapse which can lead to efficient T cell activation.[29,30]

ICAM-1 belongs to the immunoglobulin superfamily and is expressed constitutively at low levels on APC, endothelial cells, and other cell types.[16] The upregulation of ICAM-1 can be induced by inflammatory mediators such as IL-1.[31] Generally, the binding of cell adhesion molecules is enhanced by oligomerization and clustering of the adhesion molecules.[16] ICAM-1

rearranges into noncovalent homodimers on the cell surface *via* interactions between domain 4 (D4).[16] Moreover, D4−D4 dimers can then be noncovalently linked by interaction of domain 1, resulting in a "W" shaped tetramer that forms linear arrays that are likely bent into circular arrays. This organization of ICAM-1 influences formation of the immunological synapse (Figure 1).[16]

The binding of LFA-1 to ICAM-1 is also tightly regulated. The interaction of LFA-1 to ICAM-1 is driven by cluster formation and a change in LFA-1 conformation leading to higher avidity and affinity, respectively.[17] Binding of TCRs to peptide−MHC complexes generates intracellular signals leading to an increase in avidity of LFA-1 binding by forming a cluster.[17,32] The adhesion of DCs and T cells involves LFA-1 and ICAM-1 clusters made up of thousands of molecules.[16] The high densities of ICAM-1 on APCs and LFA-1 on T cells are necessary for firm, long-lasting conjugation. Thus, the nature of T cell conjugation to DCs suggests that multivalent inhibitors may pose an interesting intervention.

LABL and cIBR peptides have been shown to bind specifically to ICAM-1 and LFA-1, respectively.[19,20] These peptides also specifically bind their respective ICAM-1 and LFA-1 receptors when conjugated to nanoparticles.[23,25] Presenting these as multivalent arrays on the nanoparticle surface was hypothesized to provide more potent intervention strategies due to enhanced binding avidity, triggered endocytosis of receptors, and changes in cell response (Figure 1).[33,34]

In this study, pretreatment of DCs with LABL-NPs yielded up to a ~76% decrease in T cell conjugate formation with DCs, suggesting that LABL-NPs bound to ICAM-1 on DCs and blocked the availability of ICAM-1 to interact with LFA-1 on T cells. Similar results were obtained when DCs were pretreated with cIBR-NPs. The quantity of T cells binding to DCs treated with cIBR-NPs was reduced by 78% when compared to untreated control. LABL-NPs and cIBR-NPs blocked T cell conjugation to DCs to a greater extent than LABL peptide, cIBR peptide, anti-ICAM-1 antibody, anti-LFA-1 antibody, and unconjugated NPs.

Inhibition of T cell conjugation to DCs was most likely due to an increase in the binding avidity of multivalent peptides and perhaps internalization of cell adhesion molecules facilitated by the nanoparticles.[33,34] Multiple copies of LABL or cIBR peptide conjugated to the surface of nanoparticles were hypothesized to induce the clustering of LFA-1 and ICAM-1, hence enhancing the binding avidity of peptides to activated, high-density receptors. Welder *et al.* has shown that monovalent soluble ICAM-1 is unable to bind efficiently to LFA-1 expressing cells unless it is rendered multivalent by coupling to polystyrene microspheres.[34] Furthermore, the peptide−NPs were suspected to sustain inhibition by inducing receptor internalization. Internalization of clustered ICAM-1 on endothelial cells is known to be triggered by multimeric anti-ICAM-1 conjugated on microspheres, whereas monomeric anti-ICAM-1 was not efficiently internalized.[33] LABL-NPs and cIBR-NPs have also been shown to be internalized into lung epithelial cells and HUVEC cells expressing ICAM-1 and T cells expressing LFA-1, respectively.[23−25] Here, the punctate staining patterns observed in DCs treated with NPs indicated uptake and presumably receptor internalization.

LABL-NPs, cIBR-NPs, and NPs induced TNF-α production, which may result from endocytosis or processing of particles in DCs.[35] Indeed, PLGA nanoparticles have been shown to induce proinflammatory cytokine production and increase T cell proliferation.[36−38] Coincubation of T cells with DC that had been pretreated with untargeted NPs led to high levels of TNF-α, IL-6, and IL-17 and augmented T cell proliferation relative to untreated DCs. A similar observation was previously reported in DCs treated with PLGA microspheres.[39] LABL-NPs decreased the production of IL-6 from DCs and/or OT-II T cells and also resulted in a decrease the amount of IL-17, presumably by inhibiting T cell differentiation into Th17 cells.

DCs pretreated with cIBR-NPs also induced TNF-α production and proliferation of OT-II T cells in a dose-dependent manner. Significantly lower levels of IL-6 and IL-17 were produced when comparing cIBR-NPs to other NPs or to untreated coculture. In addition, it was unclear whether the T cells that proliferate following stimulation of T cells with cIBR-NP treated DC were Th1, Th2, or Th17 cells. On the basis of previous reports, LFA-1 does not seem to deliver a co-stimulatory signal but improves engagement of TCR by promoting adhesion of T cells to APC.[3] Blockade of LFA-1 on DCs would, therefore, not be expected to inhibit T cell activation by DCs. However, it could change the T cell differentiation by changing the microenvironment of T cell during activation. Although cIBR-NPs blocked T cell conjugation to DCs initially, this effect was most likely transient since substantial T cell proliferation was observed at day 7. Data also showed that increasing cIBR-NP dose ultimately increased T cell proliferation.

CONCLUSION

Chemical conjugation of LABL and cIBR peptides to PLGA NPs generated efficient targeting to ICAM-1 and LFA-1 receptors on DCs, respectively. LABL-NPs and cIBR-NPs were found to be effective inhibitors of T cell conjugation to DCs. LABL-NPs and cIBR-NPs blocked T cell conjugation to DCs more efficiently than untargeted NPs, free peptides, and antibodies. Compared to controls, T cell proliferation was arrested when T cells were incubated in the presence of DCs treated with LABL-NPs, whereas DCs treated with cIBR-NPs or untargeted NPs dramatically stimulated the division of T cells. These findings suggested the potential of

LABL-NPs to change the character of mature DCs, yet block immunological synapse formation without stimulating T cell proliferation and point to cIBR-NPs as inducers of T cell expansion. All NPs increased the production of TNF-α compared to free ligands or untreated controls, but the amount of IL-6 or IL-7 depended on NP type. Collectively, results suggested that LABL-NPs and cIBR-NPs function as distinct immune modulators that dramatically differ from soluble peptide inhibitors of ICAM-1 or LFA-1.

MATERIALS AND METHODS

Materials. LABL peptide (ITDGEATDSG, M_w 964.95) and cIBR peptide (cyclo 1,12 Pen-PRGGSVLVTGC, M_w 1174.50) were synthesized on a Pioneer peptide synthesizer (PerSeptive Biosystems, CA). Poly(DL-lactic-*co*-glycolic acid) (50:50) with terminal carboxyl group (PLGA, inherent viscosity 0.67dL/g, M_w ~90 kDa) was purchased from Lakeshore Biomaterials (Birmingham, AL). PluronicF-127 was obtained from BASF Corporation (Mount Olive, NJ). 1-Ethyl-3-[3-dimethylaminopropyl]carbodiimide hydrochloride (EDC), *N*-hydroxysulfosuccinimide (sulfo-NHS), and 2-β mercaptoethanol were purchased from Thermo Fisher Scientific Inc. (Rockford, IL). Coumarin-6 was purchased from Polysciences, Inc. (Warrington, PA). Dialysis membrane (M_wCO 100 000) was purchased from Spectrum Laboratory Products Inc. (Rancho Dominguez, CA). RPMI-1640 medium was obtained from Cellgro (Manassas, VA). Tumor necrosis factor-α (TNF-α) was purchased from Promega (Madison, WI, USA). Granulocyte macrophage-colony stimulating factor (GM-CSF) was purchased from Peprotech Inc. (Rocky Hill, NJ). Carboxyfluorescein diacetate succimidyl ester (CFSE) and 5-(and-6)-(((4cloromethyl) enzoyl)amino)tetramethylrhodamine (Orange CMTMR) were purchased from Invitrogen Corporation, (Carlsbad, CA). Monoclonal antihuman CD54 (ICAM-1) domain 1 and monoclonal anti-LFA-1 were purchased from Ancell (Bayport, MN). CellTiter 96 AQ_{ueous} non-radioactive cell proliferation assay (MTS) was purchased from Promega (Madison, WI). Ovalbumin was purchased from Sigma (St. Louis, MO). Penicillin, streptomycin, and L-glutamine were purchased from Cellgro (Manassas, VA). IL-2 was generously provided by Dr. Christophe Nicot at the University of Kansas Medical Center. B6.129S7-*Rag1*^{tm1Mom}Tg-(TcraTcrb)425Cbn mice were purchased from Taconic Farms (Hudson, NY). C57BL/6 wild-type mice were purchased from Jax Laboratories (Bar Harbor, ME).

Methods. *Cell Culture and Isolation.* Bone marrow derived dendritic cells were generated from C57BL/6 wild-type mice as described.[39] Briefly, 2 × 10^6 cells were isolated from bone marrow, plated on bacterial Petri dishes, and cultured in 10 mL of DC media (RPMI-1640, 10% heat inactivated fetal bovine serum, 100 μg/mL penicillin−streptomycin, 50 μM β-mercaptoethanol, 20 ng/mL murine granulocyte macrophage colony stimulating factor (GM-CSF) (R&D)), and 2 nM L-glutamine. At 72 h (day 3), 10 mL of fresh DC media was added to each dish. On days 6 and 8, 10 mL of supernatant and cells were removed, and cells recovered by centrifugation (90*g*) and added back to the dish with fresh DC medium. On day 9, non-adherent cells were collected, labeled with (5 μM) 5-(and-6)-carboxyfluorescein diacetate, succinimidyl ester (CFSE) for 10 min at 37 °C, washed, primed with 50 μg/mL ovalbumin, and matured overnight with 100 ng/mL TNF-α.

On day 10, T cells were isolated from B6.129S7-*Rag1*^{tm1Mom} Tg(TcraTcrb)425Cbn mice spleens by passing spleens through a wire mesh. T cells were purified using a negative selection, mouse T cell enrichment kit according to manufacturers' directions (EasySep).

PLGA Nanoparticle Preparation and Characterization. PLGA nanoparticles and nanoparticles loaded with coumarin-6 were prepared by a solvent displacement method. In brief, PLGA was dissolved in acetone (18 mg/mL) containing coumarin-6 (50 μg/mL). The solution was gently infused into 0.1% PluronicF-127-COOH (25 mL) under mild stirring (300 rpm). Terminal hydroxyl groups on PluronicF-127 were converted to carboxyl groups according to a reported procedure.[25,40] PluronicF-127-OH was dissolved in tetrahydrofuran. Then, 4-dimethylaminopyridine (DMAP), triethylamine, and succinic anhydride were added, and the mixture was stirred for 48 h at room temperature. The solution was dried by rotary evaporation and was then dissolved in carbon tetrachloride. The excess succinic anhydride was removed. The resulting Pluronic F-127-COOH was purified by precipitation with ice-cold diethylether. The resultant nanoparticle suspension was dialyzed (100 000 MWCO) against a 0.2% mannitol solution for 48 h to remove excess surfactant. Particle size and zeta-potential of nanoparticles were characterized using dynamic light scattering (ZetaPALS, Brookhaven Instrument Inc.).

Conjugation of LABL and cIBR Peptides to PLGA Nanoparticles. The N-terminus of peptide was covalently linked with the carboxyl groups of PluronicF-127-COOH coated on PLGA nanoparticles by carbodiimide chemistry.[23] Specific binding of the LABL and cIBR peptides suggests that they are radially pointing away from the particles' surface (Figure 1). Nanoparticles (2.2 mg/mL) were buffered using 2-(*N*-morpholino)ethanesulfonic acid (MES; pH 6.5) and incubated with 100 mM 1-ethyl-3-[3-dimethylaminopropyl]carbodiimide hydrochloride (EDC) and 50 mM *N*-hydroxysulfosuccinimide (sulfo-NHS) for 15 min. EDC was used to react with a carboxyl group on PLGA NPs and formed an amine-reactive O-acylisourea intermediate. Sulfo-NHS was added to stabilize this intermediate, hence increasing the efficiency of the coupling reaction. Excess EDC and sulfo-NHS were removed by centrifugation (16 089*g*, 10 min). Then, cIBR or LABL peptides (0.4 mg) were added and allowed to react with PluronicF-127-COOH on nanoparticles for 12 h at room temperature. Peptide-conjugated NPs were collected by centrifugation (16 089*g*, 10 min) and washed three times with purified water.

The conjugation efficiency was determined by quantifying the unconjugated ligand remaining in the reaction medium after nanoparticle separation. The peptide density on the surface of nanoparticles after reaction was calculated assuming a normal Guassian particle size distribution.[23,25] The amount of free peptides in the reaction medium was analyzed by gradient reversed phase HPLC (Shimadzu) using a C_{18} column. The HPLC consisted of SCL-10A Shimadzu system controller, LC-10AT VP Shimadzu liquid chromatography, SIL-10A XL Shimadzu autoinjecter set at 30 μL injection volume, DGU-14A Shimadzu degasser, sample cooler, and SPD-10A Shimadzu UV−vis detector (220 nm). The HPLC-UV system was controlled by a personal computer equipped with Shimadzu class VP software. All separations were carried out using a Vydac HPLC protein and peptide C_{18} column. Gradient elution was carried out to determine the amount of LABL peptide at constant flow of 1 mL/min, from 0% B to 8% B for 5 min, followed by 14.3% B at 17.5 min, 50% at 23 min, and 70% B at 24−35 min. HPLC gradient system was programmed to separate cIBR peptide at constant flow of 1 mL/min, from 25% B for 5 min, 55% B at 25 min, and 100% B at 25.1−30 min. Mobile phase compositions were (A) acetonitrile−water (5:95) with 0.1% TFA and (B) 100% acetonitrile with 0.1% trifluoroacetic acid (TFA).

LFA-1 and ICAM-1 Expression on Dendritic Cells and T Cells. The relative expression of LFA-1 and ICAM-1 on T cells and DCs was qualitatively assessed using flow cytometry (FACScan). DCs (4 × 10^5 cells/mL) were matured with TNF-α (1000 U/mL) and primed with ovalbumin (OVA) (50 μg/mL) for 24 h. DCs were isolated by centrifugation and incubated for 45 min on ice with 80 μL of anti-ICAM-1 (0.05 mg/mL) or anti-LFA-1 (0.25 mg/mL) conjugated with FITC at 1:50 dilution. Cells were washed three times and analyzed by flow cytometry.

Splenic C57BL/6-TgN(OT-II.2a)-Rag1 T cells (2.2×10^6 cells/mL) were incubated with 80 μL of anti-ICAM-1-FITC (0.05 mg/mL) or anti-LFA-1-FITC (0.25 mg/mL) on ice for 45 min. Unbound antibodies were removed by rinsing three times with PBS after centrifugation (16 089*g*, 2.5 min). The fluorescent intensity of cells was measured by a FACscan flow cytometer. Data analysis was performed using Cell Quest software (BD).

Binding and Uptake of LABL-NPs and cIBR-NPs into DCs. The binding and uptake of LABL-NPs and cIBR-NPs encapsulated fluorescent dye was monitored using flow cytometry. DCs (1×10^5 cells/mL) were added and allowed to adhere on a 96-well plate (200 μL/well) for 24 h in the presence of TNF-α (1000 U/mL) and OVA (50 μg/mL). DCs were washed three times with PBS and incubated with NPs, LABL-NPs, or cIBR-NPs (2.2 mg/mL, 100 μL) at 37 °C for 15, 30, 45, and 60 min. Cells were washed three times with PBS and trypsinized for 3 min at 37 °C. Then DCs were transferred to a microcentrifuge tube and washed once with PBS by centrifugation (600*g*, 2 min). The fluorescent intensity due to DC uptake of fluorescent NPs was measured using the FACscan flow cytometer. Data analysis was performed using Cell Quest software (BD). The fluorescent intensity of cells incubated with NPs was normalized by the fluorescent intensities of each NP formulation.

Fluorescence Microscopy of DCs Binding/Uptake with LABL-NPs or cIBR-NPs. Dendritic cells (1×10^6 cells/mL, 300 μL) were added into an 8-well plate and stimulated by TNF-α (1000 U/mL) and OVA (50 μg/mL) for 24 h. Cells were washed with PBS and then incubated with NPs, LABL-NPs, or cIBR-NPs (2.2 mg/mL, 300 μL) for 40 min at 37 °C. Unbound nanoparticles were removed by washing three times with PBS, and cells were fixed with 4% paraformaldehyde. Fluorescence micrographs were acquired using the FITC filter set of a Nikon Eclipse 80i microscope equipped for epifluorescence. Micrographs were captured using an Orca ER camera (Hamamatsu, Inc., Bridgewater, NJ) and analyzed by Metamorph, version 6.2 (Universal Imaging Corp., West Chester, PA). All images were corrected for variations in excitation light intensity.

In Vitro Cellular Cytotoxicity of LABL-NPs and cIBR-NPs. MTS cell viability assays were performed to provide an assessment of the toxicity of LABL-NPs and cIBR-NPs on T cells and TNF-α stimulated and OVA primed DCs. Briefly, T cells (3.2×10^6 cells/mL) and DCs (1×10^5 cells/mL) were seeded on 96-well plates and incubated with various concentrations of LABL-NPs and cIBR-NPs for 24 h. A tetrazolium salt MTS was applied, and the incubation was continued for an additional 4 h. MTS was converted by mitochondrial dehydrogenase enzyme in living cells to form a colored formazan product. The absorbance of the formazan product was recorded at 490 nm using a 96-well plate reader (Spectramax M5).

DCs and T Cell Conjugate Formation.[41] DCs (4×10^5 cells/mL) were stained by incubating with 5 mL of CFSE in PBS (10 μM) for 10 min at 37 °C in PBS. The staining was quenched by the addition of 25 mL of complete culture medium and incubation at 4 °C for 10 min. The remaining dye was washed away by three washes with complete culture medium. T cells were incubated with 10 μL of CMTMR orange fluorescent dye (5 μM) in 10 mL of PBS for 30 min at 37 °C. The reaction of the dye was quenched by incubating with complete culture medium for 30 min at 37 °C. T cells were washed three times with complete culture medium. Untreated DCs were used as a positive control. Dendritic cells (4×10^5 cells/mL) primed with OVA (50 μg/mL) and matured in the presence of TNF-α (1000 U/mL) were incubated with anti-ICAM-1 (1 μg/mL), anti-LFA-1 (5 μg/mL), NPs (2.2 mg/mL), LABL peptide (0.095, 0.19, and 0.38 mM), LABL-NPs (1.1, 2.2, and 4.4 mg/mL), cIBR peptide (0.012, 0.024, and 0.048 mM), or cIBR-NPs (1.1, 2.2, and 4.4 mg/mL) for 30 min at 37 °C. DCs were washed three times with PBS and incubated with T cells (2×10^6 cells/mL) for 2 h at 37 °C. After incubation, DCs were washed three times with PBS and fixed with 4% paraformaldehyde. Cells were imaged using an Orca ER camera (Hamamatsu, Inc., Bridgewater, NJ) and imaged using Metamorph, version 6.2 (Universal Imaging Corp., West Chester, PA). Dendritic cells and T cells attached to dendritic cells were measured by using ImageJ software per condition from all images. The analysis was performed by using color segmentation (RGB channel separation), which was made binary and followed by measurement of the area of R and G channels. Similar threshold limiting was applied to all images and colors. The results were reported by the percent of ratio of R channel area (corresponds to T cells) to G channel area (corresponds to DC). The percentage of T cell conjugates was calculated.

$$\%\text{T cell conjugated to DC} = \frac{\text{area of T cells binding DCs} \times 100}{\text{area of DCs}}$$

T Cell Proliferation Assay. Primary T cells isolated from C57BL/6-TgN(OT-II.2a)-Rag1 mice were labeled with carboxyfluorescein succinimidyl ester (CFSE) (5 μM) for 10 min at 37 °C, 5% CO_2, to observe the dye dilution by cell division. The staining was quenched by the addition of 5 volumes of culture medium into T cells and incubated 10 min at 4 °C. DCs (4×10^5 cells/mL) were matured in the presence of TNF-α (1000 U/mL) and primed with OVA (50 μg/mL) for 24 h in 24-well plate. DCs were treated with anti-ICAM-1 (1 μg/mL), anti-LFA-1 (5 μg/mL), unconjugated NPs (2.2 mg/mL), LABL peptide (0.095, 0.19, and 0.38 mM), LABL-NPs (1.1, 2.2, and 4.4 mg/mL), cIBR peptide (0.012, 0.024, and 0.048 mM), or cIBR-NPs (1.1, 2.2, and 4.4 mg/mL) for 30 min, at 37 °C, 5% CO_2, and washed three times with PBS. T cells (2×10^6 cells/mL) in serum-free RPMI-1640, IL-2, and 1% penicillin−streptomycin were incubated with DCs 7 days at 37 °C, 5% CO_2. T cells collected after 24 h (1 day) and 168 h (7 days) were centrifuged at 16 089*g* for 2 min and fixed with 4% paraformaldehyde. The CFSE dilution was measured by using FACScan flow cytometer. The percent of T cell proliferation was analyzed by calculating the percent of cells with diluted CFSE using FlowJo software.

Quantification of Cytokines in Cell Culture Supernatants by ELISA. DCs were matured in the presence of TNF-α (1000 U/mL) and primed with OVA (50 μg/mL) for 24 h in 24-well plate. DCs were treated with anti-ICAM-1 (1 μg/mL), anti-LFA-1 (5 μg/mL), unconjugated NPs (2.2 mg/mL), LABL peptide (0.095, 0.19, and 0.38 mM), LABL-NPs (1.1, 2.2, and 4.4 mg/mL), cIBR peptide (0.012, 0.024, and 0.048 mM), or cIBR-NPs (1.1, 2.2, and 4.4 mg/mL) for 30 min, at 37 °C, 5% CO_2, and washed three times with PBS. T cells (2×10^6 cells/mL) in serum-free RPMI-1640, IL-2, and 1% penicillin−streptomycin were incubated with DCs 7 days at 37 °C, 5% CO_2. Supernatants of cell cultures were collected for cytokine detection. Secreted TNF-α, IL-2, IL6, and IL-17 were measured by ELISA assay (Cytokine Core Lab, Baltimore, MD). ELISA was performed in Nunc Maxisorb ELISA strips freshly coated with capture antibody for 16 h before the assay was performed. Detecting antibody and the streptavidin−peroxidase conjugate were added into standard, all samples, and controls. Premixed substrate solution (Neogen) was then added. The plate was read on a Molecular Devices ELISA plate reader. Curve fitting was selected among linear, quadratic, and 4-point based on the best regression coefficient using the SoftPro software package.

Statistical Analysis. Statistical evaluation of data was performed using an analysis of variance (one-way ANOVA). Newman−Keuls was used as a posthoc test to assess the significance of differences. To compare the significance of the difference between the means of two groups, a *t*-test was performed; in all cases, a value of $p < 0.05$ was accepted as significant.

Acknowledgment. The authors acknowledge J. Krise for providing the fluorescence microscope. We would like to acknowledge support from the Royal Thai Government, the Coulter Foundation, and the Institute for Advancing Medical Innovation as well as additional lab funding from the NIH (R03 AR054035, P20 RR016443, and T32 GM08359-11) and the Department of Defense. In addition, we acknowledge the support of National Institutes of Health (R01-AI063002 and R56-AI063002), K22AI060815, and the Biomedical Research and Training Program.

Supporting Information Available: Additional supporting figure. This material is available free of charge *via* the Internet at http://pubs.acs.org.

REFERENCES AND NOTES

1. Dustin, M. L.; Shaw, A. S. Costimulation: Building an Immunological Synapse. *Science* **1999,** *283*, 649–650.

2. Dustin, M. L. T-Cell Activation through Immunological Synapses and Kinapses. *Immunol. Rev.* **2008,** *221*, 77–89.
3. Bachmann, M. F.; McKall-Faienza, K.; Schmits, R.; Bouchard, D.; Beach, J.; Speiser, D. E.; Mak, T. W.; Ohashi, P. S. Distinct Roles for LFA-1 and CD28 during Activation of Naive T Cells: Adhesion *versus* Costimulation. *Immunity* **1997,** *7*, 549–557.
4. Van Seventer, G. A.; Shimizu, Y.; Horgan, K. J.; Shaw, S. The LFA-1 Ligand ICAM-1 Provides an Important Costimulatory Signal for T Cell Receptor-Mediated Activation of Resting T Cells. *J. Immunol.* **1990,** *144*, 4579–4586.
5. Springer, T. A.; Dustin, M. L.; Kishimoto, T. K.; Marlin, S. D. The Lymphocyte Function-Associated LFA-1, CD2, and LFA-3 Molecules: Cell Adhesion Receptors of the Immune System. *Annu. Rev. Immunol.* **1987,** *5*, 223–252.
6. Lunsford, K. E.; Koester, M. A.; Eiring, A. M.; Horne, P. H.; Gao, D.; Bumgardner, G. L. Targeting LFA-1 and CD154 Suppresses the *In Vivo* Activation and Development of Cytolytic (CD4-Independent) CD8+ T Cells. *J. Immunol.* **2005,** *175*, 7855–7866.
7. Simnick, A. J.; Valencia, A.; Liu, R.; Chilkoti, A. Morphing Low-Affinity Ligands into High-Avidity Nanoparticles by Thermally Triggered Self Assembly of a Genetically Encoded Polymer. *ACS Nano* **2010,** *4*, 2217–2227.
8. Stukel, J. M.; Li, R. C.; Maynard, H. D.; Caplan, M. R. Two-Step Synthesis of Multivalent Cancer-Targeting Constructs. *Biomacromolecules* **2010,** *11*, 160–167.
9. Hong, A.; Leroueil, P. R.; Majoros, I. J.; Orr, B. G.; Baker, J. R., Jr.; Banaszak Holl, M. M. The Binding Avidity of a Nanoparticle-Based Multivalent Targeted Drug Delivery Platform. *Chem. Biol.* **2007,** *14*, 107–115.
10. Johnson, R. N.; Kopeckova, P.; Kopecek, J. Synthesis and Evaluation of Multivalent Branched HPMA Copolymer-Fab' Conjugates Targeted to the B-Cell Antigen CD20. *Bioconjugate Chem.* **2009,** *20*, 129–137.
11. Ding, H.; Prodinger, W. M.; Kopecek, J. Identification of CD21-Binding Peptides with Phage Display and Investigation of Binding Properties of HPMA Copolymer-Peptide Conjugates. *Bioconjugate Chem.* **2006,** *17*, 514–523.
12. Carlson, C. B.; Mowery, P.; Owen, R. M.; Dykhuizen, E. C.; Kiessling, L. L. Selective Tumor Cell Targeting Using Low-Affinity, Multivalent Interactions. *ACS Chem. Biol.* **2007,** *2*, 119–127.
13. Puffer, E. B.; Pontrello, J. K.; Hollenbeck, J. J.; Kink, J. A.; Kiessling, L. L. Activating B Cell Signaling with Defined Multivalent Ligands. *ACS Chem. Biol.* **2007,** *2*, 252–262.
14. Gordon, E. J.; Sanders, W. J.; Keissling, L. L. Synthetic Ligands Point to Cell Surface Strategies. *Nature* **1998,** *392*, 30–31.
15. Mowery, P.; Yang, Z. Q.; Gordon, E. J.; Dwir, O.; Spencer, A. G.; Alon, R.; Kiessling, L. L. Synthetic Glycoprotein Mimics Inhibit L-Selectin Mediated Rolling and Promote L-Selectin Shedding. *Chem. Biol.* **2004,** *11*, 725–732.
16. Lebedeva, T.; Dustin, M. L.; Sykulev, Y. ICAM-1 Co-stimulates Target Cells To Facilitate Antigen Presentation. *Curr. Opin. Immunol.* **2005,** *17*, 251–258.
17. Hogg, N.; Laschinger, M.; Giles, K.; McDowall, A. T-Cell Integrins: More Than Just Sticking Points. *J. Cell. Sci.* **2003,** *116*, 4695–4705.
18. Anderson, M. E.; Siahaan, T. J. Targeting ICAM-1/LFA-1 Interaction for Controlling Autoimmune Diseases: Designing Peptide and Small Molecule Inhibitors. *Peptides* **2003,** *24*, 487–501.
19. Anderson, M. E.; Siahaan, T. J. Mechanism of Binding and Internalization of ICAM-1-Derived Cyclic Peptides by LFA-1 on the Surface of T Cells: A Potential Method for Targeted Drug Delivery. *Pharm. Res.* **2003,** *20*, 1523–1532.
20. Jois, S. D. S.; Siahaan, T. J. A Peptide Derived from LFA-1 That Modulates T-Cell Adhesion Binds to Soluble ICAM-1 Protein. *J. Biomol. Struc. Dyn.* **2003,** *20*, 635–644.
21. Tibbetts, S. A.; Seetharama, J. D.; Siahaan, T. J.; Benedict, S. H.; Chan, M. A. Linear and Cyclic LFA-1 and ICAM-1 Peptides Inhibit T Cell Adhesion and Function. *Peptides* **2000,** *21*, 1161–1167.
22. Tibbetts, S. A.; Chirathaworn, C.; Nakashima, M.; Jois, D. S.; Siahaan, T. J.; Chan, M. A.; Benedict, S. H. Peptides Derived from ICAM-1 and LFA-1 Modulate T Cell Adhesion and Immune Function in a Mixed Lymphocyte Culture. *Transplantation* **1999,** *68*, 685–692.
23. Chittasupho, C.; Manikwar, P.; Krise, J. P.; Siahaan, T. J.; Berkland, C. cIBR Effectively Targets Nanoparticles to LFA-1 on Acute Lymphoblastic T Cells. *Mol. Pharmaceutics* **2010,** *7*, 146–155.
24. Zhang, N.; Chittasupho, C.; Duangrat, C.; Siahaan, T. J.; Berkland, C. PLGA Nanoparticle−Peptide Conjugate Effectively Targets Intercellular Cell-Adhesion Molecule-1. *Bioconjugate Chem.* **2008,** *19*, 145–152.
25. Chittasupho, C.; Xie, S.; Baoum, A.; Yakovleva, T.; Siahaan, T. J.; Berkland, C. ICAM-1 Targeting of Doxorubicin-Loaded PLGA Nanoparticles to Lung Epithelial Cells. *Eur. J. Pharm. Sci.* **2009,** *37*, 141–150.
26. Commins, S. P.; Borish, L.; Steinke, J. W. Immunologic Messenger Molecules: Cytokines, Interferons, and Chemokines. *J. Allergy Clin. Immunol.* **2010,** *125*, S53–72.
27. Zhu, J.; Yamane, H.; Paul, W. E. Differentiation of Effector CD4 T Cell Populations. *Annu. Rev. Immunol.* **2010,** *28*, 445–489.
28. Miossec, P.; Korn, T.; Kunchroo, V. K. Interleukin-17 and Type 17 Helper T Cells. *N. Engl. J. Med.* **2009,** *361*, 888–898.
29. Dustin, M. L. A Dynamic View of the Immunological Synapse. *Semin. Immunol.* **2005,** *17*, 400–410.
30. Dustin, M. L. Modular Design of Immunological Synapses and Kinapses. *Cold Spring Harbor Perspect. Biol.* **2009,** *1*, a002873.
31. Rothlein, R.; Dustin, M. L.; Marlin, S. D.; Springer, T. A. A Human Intercellular Adhesion Molecule (ICAM-1) Distinct from LFA-1. *J. Immunol.* **1986,** *137*, 1270–1274.
32. Dustin, M. L.; Springer, T. A. T-Cell Receptor Cross-Linking Transiently Stimulates Adhesiveness through LFA-1. *Nature* **1989,** *341*, 619–624.
33. Muro, S.; Wiewrodt, R.; Thomas, A.; Koniaris, L.; Albelda, S. M.; Muzykantov, V. R.; Koval, M. A Novel Endocytic Pathway Induced by Clustering Endothelial ICAM-1 or PECAM-1. *J. Cell. Sci.* **2003,** *116*, 1599–1609.
34. Welder, C. A.; Lee, D. H. S.; Takei, F. Inhibition of Cell Adhesion by Microspheres Coated with Recombinant Soluble ICAM-1. *J. Immunol.* **1993,** *150*, 2203–2210.
35. Yoshida, M.; Babensee, J. E. Molecular Aspects of Microparticle Phagocytosis by Dendritic Cells. *J. Biomater. Sci. Polym.* **2006,** *17*, 893–907.
36. Semete, B.; Booysen, L. I. J.; Kalombo, L.; Venter, J. D.; Katata, B.; Ramalapa, J. A.; Verschoor, J. A.; Swai, H. *In Vivo* Uptake and Acute Immune Response to Orally Administered Chitosan and PEG Coated PLGA Nanoparticles. *Toxicol. Appl. Pharmacol.* **2010,** *249*, 158–165.
37. Molavi, O.; Mahmud, A.; Hamdy, S.; Hung, R. W.; Lai, R.; Samuel, J.; Lavasanifar, A. Development of a Poly(D,L-lactic-*co*-glycolic acid) Nanoparticle Formulation of STAT3 Inhibitor JSI-124: Implication for Cancer Immunotherapy. *Mol. Pharmaceutics* **2009,** *7*, 364–374.
38. Steenblock, E.; Fahmy, T. M. A Comprehensive Platform for *Ex Vivo* T Cell Expansion Based on Biodegradable Polymeric Artificial Antigen Presenting Cells. *Mol. Ther.* **2008,** *16*, 765–772.
39. Lutz, M. B; Kukutsch, N.; Ogilvie, A. L; Rössner, S.; Koch, F.; Romani, N.; Schuler, G. An Advanced Culture Method for Generating Large Quantities of Highly Pure Dendritic Cells from Mouse Bone Marrow. *J. Immunol. Methods* **1999,** *223*, 77–92.
40. Guerrouache, M.; Karakasyan, C.; Gaillet, C.; Canva, M.; Millot, M. C. Immobilization of a Functionalized Poly(ethylene glycol) onto β-Cyclodextrin-Coated Surfaces by Formation of Inclusion Complexes: Application to the Coupling of Proteins. *J. Appl. Polym. Sci.* **2006,** *100*, 2362–2370.
41. Vines, C. M.; Potter, J. W.; Xu, Y.; Geahlen, R. L.; Costello, P. S.; Tybulewicz, V. L.; Lowell, C. A.; Chang, P. W.; Gresham, H. D.; Willman, C. L. Inhibition of Beta 2 Integrin Receptor and Syk Kinase Signaling in Monocytes by The Src Family Kinase Fgr. *Immunity* **2001,** *15*, 507–519.